Targeting of inducible costimulator (ICOS) expressed on alloreactive T cells down-regulates graft-versus-host disease (GVHD) and facilitates engraftment of allogeneic bone marrow (BM)

Patricia A. Taylor, Angela Panoskaltsis-Mortari, Gordon J. Freeman, Arlene H. Sharpe, Randolph J. Noelle, Alexander Y. Rudensky, Tak W. Mak, Jonathan S. Serody, and Bruce R. Blazar

Inducible costimulator (ICOS), a CD28/cytotoxic T lymphocyte antigen 4 (CTLA-4) family member, is expressed on activated T cells. ICOS ligand, a B7 family member, is constitutively expressed on B cells, macrophages, and dendritic cells and is up-regulated on antigen-presenting cells (APCs) and some nonlymphoid tissues by tumor necrosis factor α (TNFα) or lipopolysaccharide (LPS). Thus, ICOS: ICOS ligand (ICOSL) blockade could reduce alloreactive T cell–APC interactions responsible for graft-versus-host disease (GVHD) and bone marrow (BM) graft rejection. ICOS blockade, achieved with ICOS$^{-/-}$ mice or anti-ICOS monoclonal antibody (mAb) administration, resulted in significant inhibition of GVHD in multiple strain combinations whether mediated by CD4$^+$ and/or CD8$^+$ T cells, alloantigen-specific T-cell receptor (TCR) transgenic (Tg) T cells, or CD28-, T helper 1 (Th1)–, or Th2-deficient T cells. Anti-ICOS significantly delayed GVHD mortality even when mAb infusions were delayed until day 5 after transplantation. ICOS blockade reduced the number of alloantigen-specific effector cells but did not prevent their activation. Imaging of green fluorescent protein–positive (GFP$^+$) effectors indicated that ICOS blockade inhibited expansion of GVHD-causing effector T cells in secondary lymphoid and GVHD target organs. Engraftment rates were significantly higher in ICOS$^{-/-}$ versus wild-type (WT) mice receiving allogeneic BM, and ICOS blockade significantly inhibited expansion of host antidonor alloantigen-specific BM graft-rejecting T cells. These data suggest that the ICOS pathway may be a beneficial therapeutic target for GVHD inhibition, GVHD therapy, and BM graft promotion. (Blood. 2005; 105:3372-3380)

© 2005 by The American Society of Hematology

Introduction

Inducible costimulator (ICOS), a member of the CD28 superfamily, is induced on CD4$^+$ and CD8$^+$ T cells during T-cell activation.[1] ICOS ligand (ICOSL, also known as B7h) is constitutively expressed at low levels on B cells, macrophages, and dendritic cells and is up-regulated on antigen-presenting cells (APCs) and induced on some nonlymphoid tissues (including heart, lung, kidney, and testes) by tumor necrosis factor α (TNFα) or lipopolysaccharide,[2,3] often produced during graft-versus-host disease (GVHD) responses. In vitro studies indicate that ICOS stimulates production of interleukin-4 (IL-4), interferon γ (IFNγ), and especially IL-10, but not IL-2, which can occur independently of CD28 signaling.[1] It is thought that CD28 and ICOS function in concert with CD28, which is responsible for T-cell priming and early activation events and ICOS regulating effector responses.[4]

ICOS$^{-/-}$ T cells produce greatly reduced amounts of IL-2 after activation, resulting in defective T-cell proliferation.[5] Upon restimulation, differentiated ICOS$^{-/-}$ T cells fail to express IL-4 and are defective in IL-2 production, suggesting that ICOS may regulate IL-2 expression during T-cell activation and also in the effector phase.[5] Differentiated ICOS$^{-/-}$ T cells are able to produce IFNγ and IL-10.[5] ICOS$^{-/-}$ mice exhibit severely deficient T-cell–dependent humoral responses due to impaired germinal center formation and defective immunoglobulin isotype class switching.[5-8]

Several studies indicate that ICOS plays a role in solid organ graft rejection. Harada et al[9] found that ICOS blockade prolonged cardiac allograft survival, while another study demonstrated prolonged liver allograft survival.[10] Nanji et al[11] demonstrated that the addition of a blocking anti-ICOS monoclonal antibody (mAb) to cytotoxic T lymphocyte antigen 4 (CTLA-4)–immunoglobulin (Ig), anti-CD40L mAb, or rapamycin improved pancreatic islet cell allograft survival. Fewer studies have examined the role of the ICOS pathway in bone marrow transplantation (BMT), although one report demonstrated that ICOS blockade inhibited T helper 2 (Th2)–mediated chronic GVHD but exacerbated Th1-mediated acute GVHD using nonirradiated parent-into-F1 models.[12]

This report examines the role of ICOS in regulating alloreactivity as assessed in several different irradiation models of GVHD and

bone marrow (BM) graft rejection characterized by distinct patho-physiologic mechanisms. To further explore the effect of ICOS blockade on the mechanisms of GVHD and BM graft rejection, studies were performed in T-cell receptor (TCR) transgenic (Tg) systems of both disease processes. Additionally, imaging of green fluorescent protein–positive (GFP+) T-cell effectors in GVHD control mice and anti-ICOS mAb–treated mice illustrates the multiorgan involvement of GVHD and the effect of ICOS blockade on GVHD effector cell expansion and target organ infiltration. Collectively, these data indicate that the ICOS pathway plays an important role in GVHD and graft rejection and provide insights as to the mechanisms responsible for the effect of ICOS blockade on alloreactive T-cell responses.

Materials and methods

Mice

B6.C-H2bm12 (termed bm12) (H2b), B6.C-H2bm1 (termed bm1) (H2b), B10.BR (termed BR) (H2k), BALB/c signal transducer and activator of transcription 4 (STAT4)–deficient (−/−), BALB/c STAT6−/−, C57BL/6 CD28−/−, and B6 Rag−/− mice were purchased from The Jackson Laboratory (Bar Harbor, ME). C57BL/6 (termed B6) (H2b), BALB/c (H2d), and BALB/c × C57BL/6 F1 (termed CB6) mice were purchased from the National Institutes of Health (Bethesda, MD). B6 and bm12 mice (both H2b) differ at 3 amino acids due to mutations in the major histocompatibility complex (MHC) class II IA region. B6 and bm1 mice (both H2b) differ at one amino acid in the MHC class I K region. ICOS−/− mice,[13] on the B6 background, were obtained from Dr Tak Mak (Advanced Medical Discovery Institute, Toronto, ON, Canada) and bred at the University of Minnesota (Minneapolis, MN). GFP Tg mice, on the B6 background, were obtained from the laboratory of Dr Jonathan Serody (University of North Carolina, Chapel Hill, NC). B6 TEa CD4+ TCR Tg mice[14] express a TCR that recognizes the peptide ASFEAQGLANIAVDKA from the α-chain of I-E class II molecules expressed in all APCs from H2b/I-E+ strains in the context of I-Ab and were obtained from Dr Randolph Noelle (Dartmouth Medical School, Lebanon, NH). B6 2C CD8+ TCR Tg mice[15] express a TCR that recognizes QLSPFPFDL (QL9) peptide bound to class I Ld and were obtained from Dr Matthew Mescher (University of Minnesota, Minneapolis, MN). All Tg mice were bred at the University of Minnesota. TEa GFP and 2C GFP double Tg mice, obtained by mating parental strains, were generated at the University of Minnesota. Mice were used at 6 to 14 weeks of age. All mice were housed in a specific pathogen-free facility in microisolator cages.

GVHD induction

Bm12, bm1, and CB6 mice were sublethally irradiated with 6.0 to 6.5 Gy (137Cs) total body irradiation (TBI) 4 hours before cell infusion. Bm12 and bm1 mice were infused intravenously with purified CD4+ or CD8+ T cells, respectively, from class II– or class I–disparate, respectively, B6 or B6 ICOS−/− mice. In order to obtain a more uniform effector population, CD4+ T cells were further depleted of CD25+ regulatory cells that have been shown to inhibit GVHD responses.[16,17] T cells were purified as previously described[18] and verified by flow cytometric phenotyping to be more than 95% of the desired phenotype. In other experiments, BR or B6 mice were lethally irradiated with 8.0 to 9.0 Gy by x-ray on the day prior to transplantation with 20 × 10^6 allogeneic, T-cell–depleted (TCD) BM cells and whole splenocytes from the designated strain at the indicated cell number. In a Tg model of GVHD,[19] sublethally irradiated CB6 mice were infused with lymph node (LN) cells from 2C and TEa mice adjusted for Tg CD8+ and CD4+ T-cell content (4 × 10^6 Tg T cells each). In the case of experiments comparing survival of recipients receiving wild-type versus gene-deficient splenocytes, splenic phenotyping determined that CD4+ and CD8+ T-cell proportions and ratios were similar among donor spleens (not shown). In some experiments, irrelevant rat IgG (rIgG; Rockland, Gilberts-ville, PA) or anti-ICOS mAb (hybridoma 7E.17G9.G1, rIgG2b;[6] produced

at National Cell Culture, Minneapolis, MN) was administered intraperitone-ally at a dosage of 200 μg daily from days −1 through +5, then 3 times weekly until day 28 after BMT unless otherwise indicated. Mice were monitored daily for survival and weighed twice weekly for the first month, then once weekly thereafter as well as examined for the clinical appearance of GVHD. In some experiments, representative long-term survivors were electively killed and hematoxylin and eosin–stained slides of liver, lung, colon, skin, and spleen were histologically assessed using a semiquantita-tive GVHD scoring system (0 to 4.0 grades in 0.5 increments) as published.[20] Coded sections were graded by one of us (A.P.-M.) without knowledge of the treatment.

Assessment of anti-ICOS mAb on alloantigen-specific T-cell expansion and phenotype in vivo

To determine effect of anti-ICOS on alloantigen-specific T-cell expansion and activation status, TEa and 2C LN cells (adjusted for 4 × 10^6 Tg T cells each) were infused into sublethally irradiated CB6 mice and rIgG or anti-ICOS was administered. Spleens were harvested on day 4 and Tg T cells were enumerated and activation status assessed by flow cytometry. TEa Tg T cells were identified with fluorochrome-conjugated mAb to CD4 and Vα2 and 2C Tg T cells were identified using conjugated mAb to CD8 and the anticlonotypic mAb 1B2. Activation status of Tg T cells was assessed by directly labeled fluorochromes to anti-CD25, -ICOS, -CD28, –L Sel, -CD44, -CD122 (IL-2Rβ), -CD127 (IL-7Rα), and isotype controls (Pharmingen, San Diego, CA) and analyzed using CellQuest software on a FACSCalibur flow cytometer (Becton Dickinson, Mountain View, CA). Intracellular granzyme B was assessed using Cytofix/Cytoperm kit (Pharm-ingen) and murine cross-reactive antihuman granzyme B phycoerythrin (PE; Caltag Laboratories, Burlingame, CA).[21]

In vivo imaging

Images were taken with a Magnafire color camera and software (Optronics, Goleta, CA) or a Retiga Exi color camera and QCapture software (Qimaging, Burnaby, BC) mounted onto a Leica MZFLIII stereomicro-scope using a GFP2- or a GFP2/dsRED-bandpass filter and a × 0.63 transfer lens (Leica Microsystems, Bannockburn, IL).[22] Zoom factors from × 1.0 to × 10 were used. Imaging composites were made in Photoshop (Adobe). In one imaging model, purified 2C GFP+ CD8+ and TEa GFP+ CD4+ T cells (2 × 10^6 each) were infused into sublethally irradiated CB6 recipients. In the other imaging model, purified B6 GFP+ T cells (3 × 10^6) were infused with non-GFP B6 BM into lethally irradiated BR mice. Exposure times for each organ were optimized for GVHD control mice receiving rIgG, and identical times were used for all other groups. Mice receiving allogeneic BM only (non-GFP) served as concurrent negative controls for background autofluorescence (only dark images were seen as previously reported) (data not shown). To obtain optimal images, mice were killed and dissected for imaging. There were 3 mice per group examined at 1 and 2 (and 3 weeks for non-Tg GVHD model) weeks after BMT. Imaging of mice in Tg GVHD model on day 4 was determined to be suboptimal for detection of widespread effector expansion and trafficking (data not shown). Mice within a group yielded very similar results at each time point so a representative image is illustrated.

Engraftment/rejection models

B6 wild-type (WT) and B6 ICOS−/− mice were sublethally irradiated with 5.5 Gy TBI by x-ray on the day prior to transplantation with 10 × 10^6 TCD BALB/c BM cells. Survival was monitored daily, and mice were weighed twice weekly for the first month after transplantation, then once weekly thereafter. Documentation of donor chimerism was done by phenotyping of peripheral blood leukocytes (PBLs) obtained by retro-orbital venipuncture at 6 weeks and 5 months after transplantation. Cells were stained with fluorochrome-conjugated antibodies (anti-CD8, -CD4, –MAC-1, -CD19, -H2d, -H2b, and isotype controls; Pharmingen) and analyzed using CellQuest software on a FACSCalibur flow cytometer (Becton Dickinson).

A new model to determine effect of ICOS blockade on BM graft rejection by antigen-specific host T cells was established. TEa and 2C LN cells (10 × 10^6 each) were adoptively transferred into B6 Rag−/− mice on

day −2. Mice were irradiated with 2.0 Gy TBI by x-ray on day −1 and cohorts infused with 40×10^6 BALB/c BM cells on day 0. Rat IgG or anti-ICOS mAb was infused from days −1 to +9. Spleens were harvested on day 10 and numbers of Tg TEa CD4+ and 2C CD8+ cells were determined by flow cytometric analysis.

Statistics

Survival data in GVHD experiments were analyzed by life-table methods, and actuarial survival rates are shown. Group comparisons were made by log-rank test statistics. P less than .05 was considered significant. Group comparisons of GVHD scores and total splenic effector CD4+ and CD8+ T cells were analyzed by Student t test. P less than .05 was considered significant. To assess engraftment data, group comparisons of percent donor chimerism were analyzed by Student t test. Group comparisons of rates of engraftment were analyzed by chi^2 test. P less than .05 was considered significant.

Results

ICOS regulates GVHD mediated by CD4+ or CD8+ T cells

Initial experiments evaluated the role of ICOS in GVHD models mediated solely by CD4+ or CD8+ T cells. To determine whether ICOS played a role in alloresponses mediated by only CD4+ T cells, bm12 mice were sublethally irradiated and infused with 2 different doses of purified CD25-depleted CD4+ T cells from B6 WT or ICOS$^{-/-}$ donors (Figure 1A). All recipients of WT CD4+ cells died within 25 days after transfer of cells. In contrast, 50% of recipients of 3×10^4 and 13% of 10^5 ICOS$^{-/-}$ CD4+ cells survived long-term ($P \leq .007$ vs WT at same dose). To determine whether ICOS played a role in a GVHD model mediated solely by CD8+ T

cells, bm1 mice were sublethally irradiated and infused with purified CD8+ T cells from B6 WT or ICOS$^{-/-}$ donors (Figure 1B). By 3 weeks after transfer of WT CD8+ T cells, 56% of recipients died of GVHD. In contrast, only 11% of recipients of ICOS$^{-/-}$ CD8+ T cells died of GVHD ($P = .002$). These data indicated that ICOS plays a role in alloresponses mediated by both CD4+ and CD8+ T cells. The role of ICOS was next evaluated in an MHC class I + II–disparate GVHD model mediated by both CD4+ and CD8+ T cells. BR mice were lethally irradiated and infused with B6 BM and 3 different doses of splenocytes from either B6 WT or B6 ICOS$^{-/-}$ mice (Figure 1C). Recipients of ICOS$^{-/-}$ splenocytes had significantly increased survival compared with recipients of WT splenocytes at all 3 cell doses ($P \leq .0001$). At the lowest cell dose, median survival time (MST) of recipients of WT spleen was 30 days versus 75 days for recipients of ICOS$^{-/-}$ spleen. At the highest cell dose, MST for recipients of WT vs ICOS$^{-/-}$ spleen was 21 vs 30 days, respectively (Figure 1C). Long-term survivors of ICOS$^{-/-}$ spleen had clinical evidence of GVHD (weight loss, generalized erythema of the skin, poor fur quality, hunched posture, and diarrhea).

Although the substantially reduced capacity of ICOS$^{-/-}$ effectors to mediate GVHD indicated that the ICOS pathway is an important regulator of GVHD responses, we also tested the effect of a blocking anti-ICOS mAb. BR mice were lethally irradiated and infused with B6 BM and 2 different doses of whole splenocytes. Rat IgG or anti-ICOS mAb was infused from day −1 to day +28 (Figure 1D). The administration of anti-ICOS mAb significantly prolonged survival at both cell doses (Figure 1D, rIgG vs anti-ICOS; MST of 26 vs 80 days at 15×10^6 spleen cells; 9 vs 40 days at 25×10^6 spleen cells; $P < .0001$) to a similar degree as the use
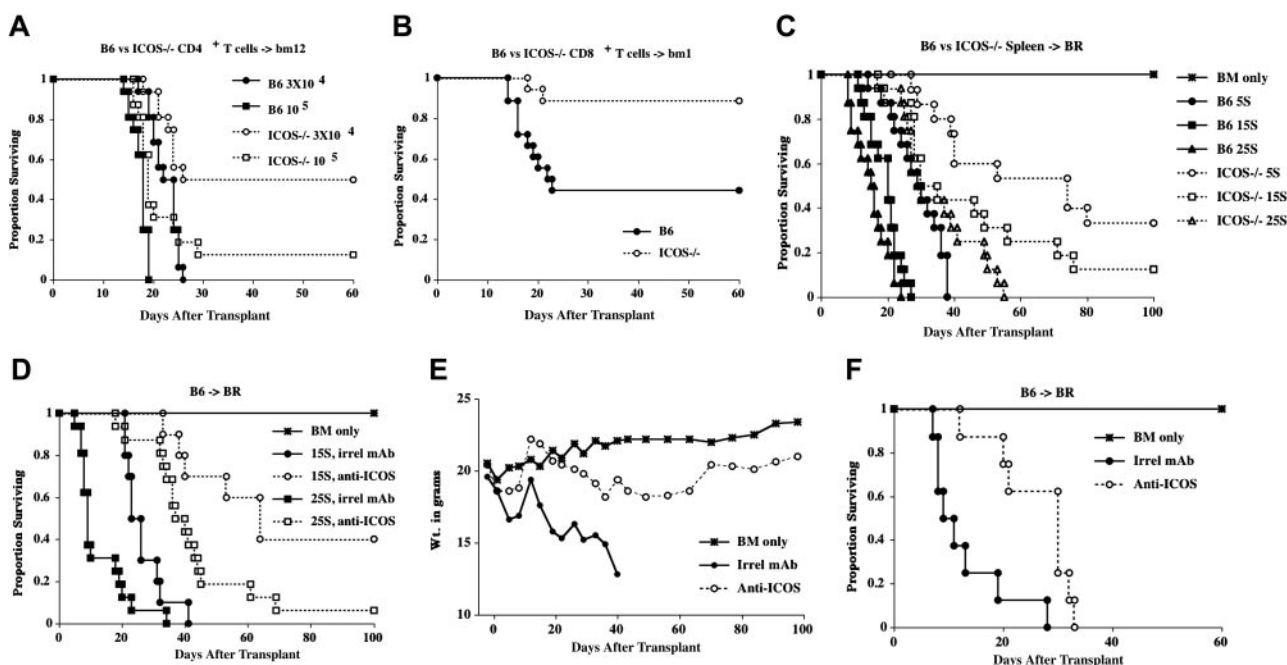
Figure 1. ICOS blockade inhibits GVHD. (A) Sublethally irradiated (6.0 Gy Cs) bm12 mice were infused with the indicated number of purified CD25-depleted CD4+ T cells from B6 WT (●, 3×10^4 cells; ■, 10^5) or B6 ICOS$^{-/-}$ mice (○, 3×10^4 cells; □, 10^5). Survival is shown (n = 16/group, pool of 2 experiments; $P = .001$ for 3×10^4 cells, $P = .007$ for 10^5 cells). (B) Sublethally irradiated (6.0 Gy Cs) bm1 mice were infused with 10^6 purified CD25-depleted CD8+ T cells from B6 WT (●) or B6 ICOS$^{-/-}$ mice (○). Survival is shown (n = 18/group, pool of 2 experiments; $P = .002$). (C) Lethally irradiated (8.0 Gy) BR mice received 20×10^6 B6 WT BM (*) and either 5×10^6, 15×10^6, or 25×10^6 splenocytes (indicated as 5S [circles], 15S [squares], or 25S [triangles], respectively) from B6 WT (filled symbols) or B6 ICOS$^{-/-}$ mice (open symbols). Survival is shown (n = 16/group, pool of 2 experiments; $P \leq .0001$, B6 vs ICOS$^{-/-}$ at each spleen dose). (D) Lethally irradiated (8.0 Gy) BR mice received 20×10^6 B6 BM (*) and either 15×10^6 or 25×10^6 B6 splenocytes (indicated as 15S [circles] or 25S [squares], respectively). Irrelevant rIgG (filled symbols) or anti-ICOS mAb (open symbols) was administered from day −1 as indicated in "Materials and methods." Survival is shown (n = 10-16 mice/group, 1 experiment for 25S, pool of 2 experiments for 15S and BM only; $P \leq .0006$, irrel mAb vs anti-ICOS at each spleen dose). (E) Average weights are shown for mice from panel D receiving 15×10^6 splenocytes (*, BM only; ●, irrelevant mAb; ○, anti-ICOS). (F) Lethally irradiated (8.0 Gy) BR mice received 20×10^6 B6 BM (*) and 25×10^6 B6 splenocytes, and rIgG (irrel mAb, ●) or anti-ICOS (○) was administered starting day 5 after transplantation. Survival is shown (n = 8/group; $P = .002$).

of ICOS$^{-/-}$ donors (compare Figure 1D with 1C). Evaluation of weight curves of mice receiving 15×10^6 spleen cells (Figure 1E) revealed that although anti-ICOS mAb–treated mice had weights superior to rIgG-treated mice, their weights were lower than those of controls that received only TCD BM, indicating that mice had sublethal GVHD. Histologic examination of GVHD target organs at 4 months after BMT also indicated that anti-ICOS mAb–treated survivors had significantly more GVHD pathology than BM-only controls in colon (infiltrates in intermucosal area with some displacement of mucosa), liver (large perivascular infiltrates associated with bile ducts and small necrotic lesions), and spleen (disruption of splenic architecture) (Table 1, experiment 1).

Anti-ICOS mAb delays GVHD mortality even when initiated after T-cell priming

It is thought that CD28 and ICOS function in concert with CD28, which is responsible for T-cell priming and early activation events and ICOS-regulating effector function at a later stage of activation. Therefore, we examined the effect of delaying anti-ICOS mAb
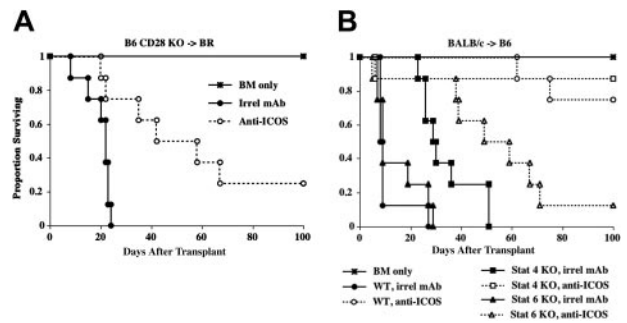

Figure 2. ICOS blockade inhibits GVHD independent of CD28, STAT4, or STAT6 signaling. (A) Lethally irradiated (8.0 Gy) BR mice received 20×10^6 B6 BM (*) and 15×10^6 B6 CD28$^{-/-}$ splenocytes. Irrelevant rIgG (●) or anti-ICOS (○) was administered from day −1 through day 28. Survival is shown (n = 8/group; P = .009). KO indicates knock out. (B) Lethally irradiated B6 (9.0 Gy) mice received 20×10^6 BALB/c BM (*) and 25×10^6 splenocytes from BALB/c WT (circles), STAT4$^{-/-}$ (squares), or STAT6$^{-/-}$ mice (triangles). Irrelevant mAb (filled symbols) or anti-ICOS (open symbols) was administered from day −1 through day 28. Survival is shown (n = 8/group; $P \leq$ .0075, irrel mAb vs anti-ICOS for each spleen donor).

Table 1. Long-term survivors of anti-ICOS mAb have sublethal GVHD

Organ	Experiment 1		Experiment 2	
	BM only	Anti-ICOS	Rad control	Anti-ICOS
Colon				
Mouse 1	1	2	1	1.5
Mouse 2	1	1.5	1.5	1
Mouse 3	1	2	1	2
Mouse 4	1	2	1.5	3
Average GVHD score ± SD	1.0 ± 0.00	1.9 ± 0.25*	1.3 ± 0.29	1.9 ± 0.85
Liver				
Mouse 1	3	3	0.5	3
Mouse 2	2	3.5	0.5	0.5
Mouse 3	1	3	0	2
Mouse 4	1.5	3.5	0.5	2
Average GVHD score ± SD	1.9 ± 0.85	3.3 ± 0.29*	0.4 ± 0.25	1.9 ± 1.03*
Lung				
Mouse 1	3	2	1	2
Mouse 2	2	3.5	1	1
Mouse 3	2.5	3	0.5	3
Mouse 4	2	3.5	0.5	2.5
Average GVHD score ± SD	2.4 ± 0.48	3.0 ± 0.71	0.8 ± 0.29	2.1 ± 0.85*
Skin				
Mouse 1	0.5	0.5	0.5	0
Mouse 2	1	0.5	0.5	0
Mouse 3	1	1.5	0.5	0.5
Mouse 4	0.5	1	0.5	0.5
Average GVHD score ± SD	0.8 ± 0.29	0.9 ± 0.48	0.5 ± 0.00	0.3 ± 0.29
Spleen				
Mouse 1	1.5	2.5	0.5	2
Mouse 2	2	3	0.5	1
Mouse 3	1	3	0.5	1
Mouse 4	0.5	3.5	0.5	1
Average GVHD score ± SD	1.3 ± 0.65	3.0 ± 0.41*	0.5 ± 0.00	1.3 ± 0.50*

GVHD target tissues were harvested 4 months (experiment 1) and 7 months (experiment 2) from 4 surviving mice per group from the experiments graphed in Figure 1D (experiment 1) and Figure 3A (experiment 2). Tissues were sectioned and stained with hematoxylin and eosin and scored for GVHD histopathology. Shown are individual and average scores out of a maximum score of 4.0.

*$P \leq$ .03.

Rad represents radiation.

until day 5 after transplantation, a time when donor antihost T-cell activation and massive T-cell proliferation have occurred and GVHD inhibition has historically been difficult to achieve. Delayed administration of anti-ICOS mAb significantly increased MST from 11 days to 30.5 days (Figure 1F, P = .0024), similar to the increase in MST seen when anti-ICOS infusions were initiated on day −1 (9 days vs 40 days, rIgG vs anti-ICOS, Figure 1D, 25×10^6 spleen dose).

ICOS blockade inhibits GVHD in the absence of CD28, STAT4, or STAT6 signaling

Because of the crucial role of the CD28:B7 costimulatory pathway in T-cell activation and effector function acquisition, we asked whether the ICOS pathway would play a role in GVHD regulation in the absence of CD28 signaling (Figure 2A). Lethally irradiated BR recipients received B6 BM and B6 CD28$^{-/-}$ splenocytes, and rIgG or anti-ICOS mAb was administered. Anti-ICOS extended the MST from 22 to 58 days (P = .009), indicating that the ICOS pathway played a major role in alloresponses even in the absence of CD28 (Figure 2A).

ICOS has been reported to play a pivotal costimulatory role in Th1/Th2 differentiation. Because optimal GVHD has been reported to require both Th1 and Th2 cells,[23] amelioration of GVHD by ICOS blockade could be the result of specific Th skewing. To determine whether ICOS blockade inhibited GVHD mediated by either Th1 or Th2 T cells, lethally irradiated B6 mice received BALB/c BM and splenocytes from either BALB/c WT, STAT4$^{-/-}$, or STAT6$^{-/-}$ mice (Figure 2B). Whereas 7 of 8 rIgG-treated mice receiving WT splenocytes died by day 10, anti-ICOS treatment resulted in long-term (day 100) survival in 6 of 8 mice reproducing the protective effect of ICOS blockade in a second strain combination that is disparate at multiple minor as well as MHC class I and II antigens (P = .0002). ICOS blockade of mice receiving STAT4$^{-/-}$ splenocytes resulted in long-term survival in 7 of 8 mice, while all rIgG-treated mice died by day 50 (P = .001). Although ICOS blockade resulted in only one long-term survivor of STAT 6$^{-/-}$ splenocytes, MST was significantly extended to 59 days versus 15 days for rIgG-treated controls (P = .0075). These data indicate that ICOS blockade significantly inhibited GVHD mediated by either Th1 or Th2 T cells, although a greater survival benefit was observed by ICOS blockade in a setting of an intact STAT6 (Th2) signaling pathway.

Anti-ICOS mAb blocks expansion, but not activation, of alloantigen-specific cells

To determine the effect of anti-ICOS mAb on alloantigen-specific T cells, 2C and TEa LN cells were infused into sublethally irradiated CB6 recipients and rIgG or anti-ICOS was administered (Figure 3A). All rIgG-treated mice died by day 21. In contrast, 7 of 8 anti-ICOS–treated mice survived long term ($P = .0002$ vs rIgG controls). Despite the profound survival advantage, anti-ICOS–treated mice had clinical evidence of GVHD at 5 months as evidenced by generalized erythema, poor fur quality, diarrhea, hunched posture, and a 20% weight reduction compared with irradiated control mice that did not receive Tg LN cells (data not shown). Evaluation of GVHD target tissues revealed significant GVHD pathology of liver (large perivascular infiltrates associated with bile ducts), lung (perivascular and peribronchiolar cuffing), and spleen (disruption of splenic architecture and increased neutrophil infiltration) in anti-ICOS–treated survivors compared with irradiated control mice (Table 1, experiment 2).

To evaluate the effect of ICOS blockade on activation and expansion of alloantigen-specific Tg T cells, 2C Tg $CD8^+$ and TEa Tg $CD4^+$ T cells, recovered from the spleens of irradiated host CB6 mice, were enumerated and phenotyped 4 days after Tg LN transfer (Figure 3B). Anti-ICOS reduced the number of 2C $CD8^+$ and TEa $CD4^+$ Tg T cells by 63% and 26%, respectively ($P = .0027$ for $CD8^+$ and $P = .0062$ for $CD4^+$ T cells; rIgG vs anti-ICOS). ICOS was expressed at high levels on all Tg $CD8^+$ and $CD4^+$ T cells recovered from rIgG-treated controls. In contrast, ICOS expression was reduced approximately 10-fold in T cells from anti-ICOS mAb–treated mice (Figure 3C, top histograms, bold line illustrates anti-ICOS, thin solid line illustrates rIgG). Analysis of several cell surface activation antigens and intracellular expression of the cytotoxic effector molecule, granzyme B, all indicated that ICOS blockade did not inhibit the in vivo activation of alloantigen-specific Tg T cells (Figure 3C). CD28, CD25, CD44, CD122, CD127, and CD69 were significantly up-regulated and L Sel was down-regulated in both rIgG- and anti-ICOS–treated mice (albeit to slightly different degrees for CD28, CD25, and CD127),

indicative of a high degree of activation (Figure 3C; CD69 not shown). Moreover, the cytotoxic molecule granzyme B was detected intracellularly at high levels in Tg $CD8^+$ T cells recovered from rIgG-treated controls ($27\% \pm 3\%$, average $\pm$ 1 SD) and anti-ICOS–treated mice ($29\% \pm 5\%$). Also indicative of activation, flow cytometric forward and side scatter parameters were consistently higher in both Tg $CD8^+$ and Tg $CD4^+$ cells in anti-ICOS–treated mice versus rIgG-treated controls (data not shown, $P \leq .004$).

Anti-ICOS reduces the number of effector T cells in some lymphoid organs and GVHD target organs early after transplantation

To further investigate the effect of ICOS blockade on effector T-cell infiltration to GVHD target organs, in vivo imaging studies with enhanced GFP^+ effector T cells were performed. We sought to combine the power of antigen specificity of alloreactive TCR Tg T cells with GFP whole-body imaging to permit the visualization of expansion and migration of antigen-specific T cells. Therefore, we crossed B6 2C and B6 TEa mice with B6 GFP Tg mice to obtain mice that expressed both the relevant TCR and GFP transgenes to allow for tracking of alloantigen-specific T cells in vivo. Purified 2C GFP^+ $CD8^+$ and TEa GFP^+ $CD4^+$ Tg T cells were infused into sublethally irradiated CB6 mice, administered rIgG or anti-ICOS, and cohorts were imaged at 1 and 2 weeks (Figure 4, left panels). GFP^+ cells were most profoundly reduced in the small (ileum), but not the large (colon), intestine, and the skin at both time points in anti-ICOS–treated mice. A transient inhibition of GFP^+ cell infiltration into other GVHD target organs (liver, lung, and spleen) was observed at 1 week, but not 2 weeks, after transplantation. Strikingly, ICOS blockade had no discernable influence on the infiltration of GFP^+ T cells into the putative sites of GVHD initiation, LNs, or Peyer patches, at either time point.

To determine whether similar imaging findings would be observed in a polyclonal model of GVHD, studies were performed in which lethally irradiated BR mice were infused with non-GFP B6 BM and purified B6 GFP^+ T cells, given rIgG or anti-ICOS
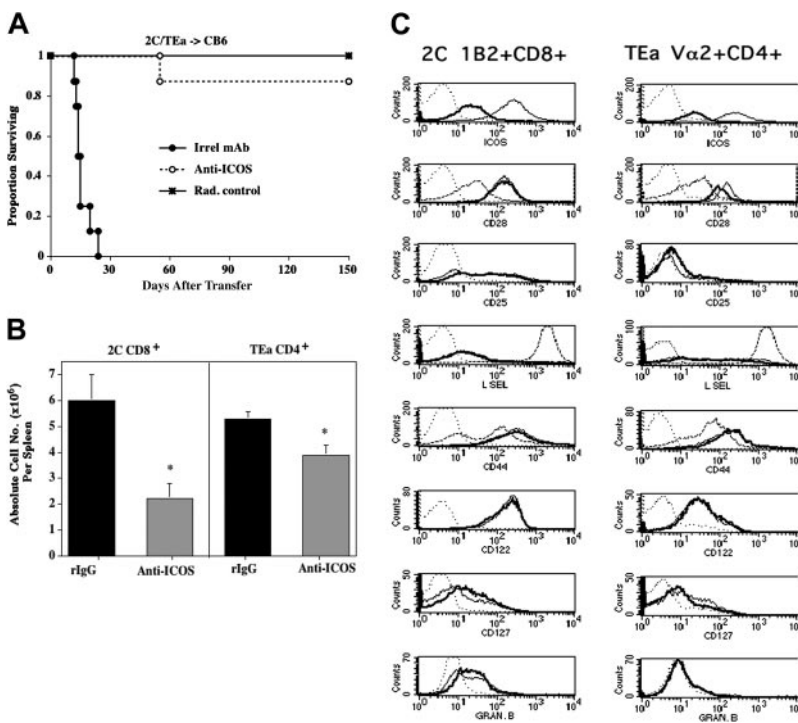
Figure 3. Anti-ICOS inhibits GVHD mediated by alloantigen-specific Tg T cells. (A) CB6 mice were sublethally irradiated (6.5 cGy Cs), infused with 2C and TEa LN adjusted for Tg T-cell content (4×10^6 T cells each), and irrelevant mAb (●) or anti-ICOS (○) was administered from day −1 through day +28. Radiation controls (*) did not receive Tg T cells or Ab. Survival is shown (n = 8/group; $P = .0002$, irrel mAb vs anti-ICOS). (B) Spleens were harvested from mice described in panel A on day 4, counted, and proportion of Tg T cells was determined by flow cytometric analysis. Shown is average of absolute counts of 2C $CD8^+$ (left) and TEa $CD4^+$ Tg T cells (right) per spleen ± 1 SEM (n = 19/group, pool of 4 separate experiments; $P = .0027$ for 2C $CD8^+$, $P = .0062$ for TEa $CD4^+$, rIgG, ■, vs anti-ICOS, ▨). (C) Spleens from mice treated as described in panels A-B were phenotyped for indicated cell surface activation antigens and intracellular cytotoxic effector molecule (granzyme B). 2C (left column) and TEa Tg cells (right column) were gated on to obtain histograms. Dotted line indicates negative control. Bold solid line and thin solid line indicate anti-ICOS and rIgG treatment, respectively. The dashed line shown in the CD28, L Sel, and CD44 histograms indicates the level of expression on freshly harvested Tg T cells. Shown is a representative sample.
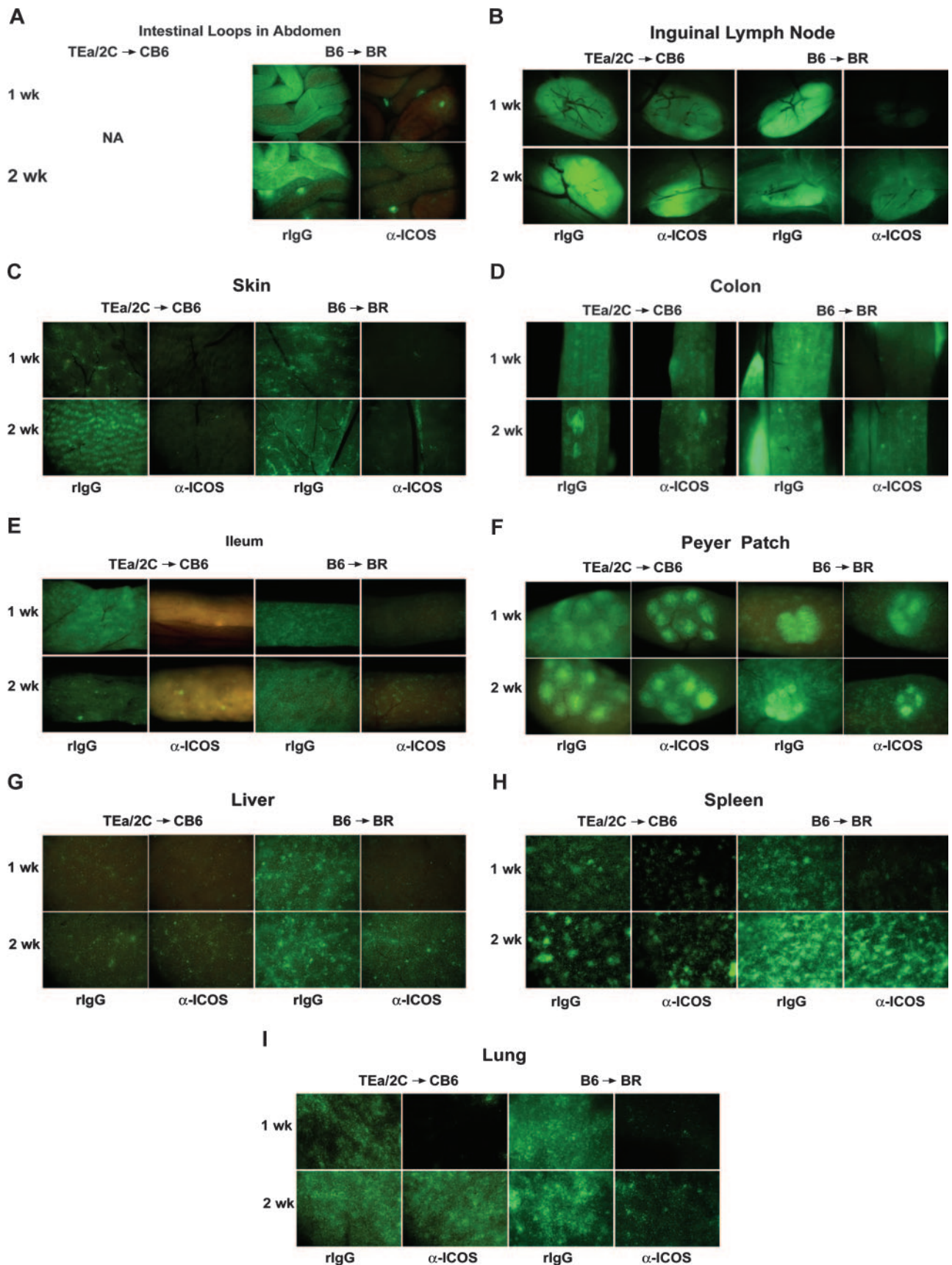
Figure 4. ICOS blockade inhibits expansion of GFP⁺ effectors in secondary lymphoid organs and GVHD target tissues. Effect of ICOS blockade in both a Tg and a polyclonal GVHD model is shown. Images of sublethally irradiated (6.5 Gy by ^{137}Cs) CB6 mice infused with purified 2C GFP⁺ CD8⁺ and TEa GFP⁺ CD4⁺ T cells (2×10^6 each) are shown in left-hand panels of each organ. Images of lethally irradiated (8.0 Gy) BR mice infused with B6 non-GFP BM (20×10^6) and purified B6 GFP⁺ T cells (3×10^6) are shown in right-hand panels of each organ. Rat IgG or anti-ICOS mAb was administered. Representative images from 1 of 3 mice per group imaged at 1 and 2 weeks are shown. Stereomicroscope was set to $\times 1.0$ zoom factor for intestinal loops in abdomen (A); $\times 3.2$ for inguinal LN (B), skin (C), colon (D), and ileum (E); $\times 4.5$ for Peyer patch (F); $\times 7.0$ for liver (G) and spleen (H); and $\times 10.0$ for lung (I). Exposure times were optimized for rIgG-treated mice for each organ and identical times were used for anti-ICOS–treated mice. Control mice not receiving GFP⁺ effectors to verify lack of autofluorescence resulted in dark images (not shown). NA indicates not available.

mAb, and imaged at 1, 2, and 3 weeks (Figure 4, right panels and data not shown). Survival studies indicated that anti-ICOS mAb administration resulted in significant inhibition of GVHD in this strain combination (Figure 1C) as well as in the Tg GVHD model (Figure 2A). Similar to the Tg GVHD model, anti-ICOS resulted in the most profound and sustained reduction of polyclonal GFP⁺ effectors in ileum and skin (Figure 4). The widespread intestinal infiltration of GFP⁺ effectors is best illustrated by the low zoom image of the loops of small intestine in the abdomen. By 1 week, the small intestine is diffusely infiltrated with GFP⁺ effectors in rIgG-treated mice. Anti-ICOS mAb profoundly reduced this infiltrative process, although GFP⁺ infiltration increased from 1 to 2 weeks in both groups of mice, indicating that anti-ICOS mAb inhibited, but did not prevent, donor T-cell expansion. As in the TCR Tg model, anti-ICOS mAb reduced GFP⁺ cells in the liver, lung, and spleen, although such reductions were more profound at 1 versus 2 weeks. A slight decrease was also noted in the colon and Peyer patches. In contrast to the TCR Tg model, GFP⁺ T cells were transiently reduced at 1 week in the LNs. Thus the dominant effects of anti-ICOS mAb administration involved the small intestine and skin with more modest and transient effects on the liver, lung, and spleen and variable effects on other secondary lymphoid organs.

ICOS pathway plays a role in graft rejection

To investigate the role of ICOS pathway in host antidonor T-cell–mediated BM graft rejection, B6 WT and B6 ICOS⁻/⁻ mice were sublethally irradiated and infused with allogeneic TCD BALB/c BM. PBLs were phenotyped 6 weeks after transplantation for determination of percentage donor chimerism (Table 2). Engraftment rates of WT and ICOS⁻/⁻ mice were 55% and 100%, respectively (*P* = .000 65). Average percentage donor chimerism in WT and ICOS⁻/⁻ was 29% and 61%, respectively (*P* = .000 19). Engraftment was stable, multilineage, and long term (> 4 months), and donor chimerism increased over time in ICOS⁻/⁻ recipients (Table 2). These data indicated that ICOS⁻/⁻ host T cells were less competent graft-rejecting effectors than WT host T cells and implicated the ICOS pathway in BM graft rejection.

A new TCR Tg rejection model was devised to further investigate the effect of ICOS blockade on alloantigen-specific rejection of donor BM. While not a model of long-term engraftment, it complements chimerism assays by permitting the direct measurement of antigen-specific host antidonor T-cell responses. On day −2, B6 TEa and 2C LN cells (10 × 10⁶ each) were adoptively transferred into syngeneic B6 Rag⁻/⁻ mice. The mice were sublethally irradiated on day −1 (2.0 Gy), infused with allogeneic BALB/c BM on day 0, and administered rIgG or anti-ICOS. Controls included mice that received the adoptive transfer of 2C/TEa LN and irradiation but not BALB/c BM. On day 10, spleens were harvested and the number and activation status of Tg T cells were determined (Figure 5 and data not shown). In the absence of BM transfer, only very low numbers of Tg T cells were
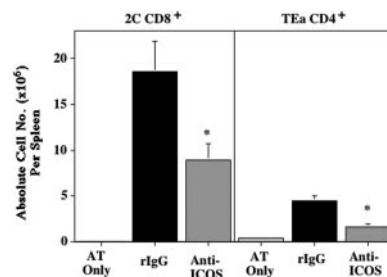
Figure 5. ICOS blockade blocks expansion of alloantigen-specific BM graft-rejecting cells. 2C and TEa LN cells (10 × 10⁶ each) were adoptively transferred into B6 Rag⁻/⁻ mice on day −2, irradiated on day −1 (2.0 Gy), infused with BALB/c BM (40 × 10⁶) on day 0, and administered rIgG or anti-ICOS mAb from day −1 to day +9. Control of irradiated mice receiving adoptive transfer of 2C and TEa LN, but not BALB/c BM, is also shown (designated as AT Only). On day 10, spleens were harvested and the number of Tg T cells was determined. Shown is average absolute number of CD8⁺ (left) and CD4⁺ Tg T cells (right) per spleen ± 1 SEM (n = 10/group, pool of 2 experiments; * indicates statistical significance. *P* = .0197 for 2C Tg CD8⁺ cells, *P* = .0006 for TEa Tg CD4⁺ cells; rIgG vs anti-ICOS).

detected (average of 4.8 × 10⁴ 2C CD8⁺ cells, 4.1 × 10⁵ TEa CD4⁺ cells), indicating that Tg T cells did not expand in the absence of relevant alloantigen. In contrast, there was a 387- and 11-fold increase of Tg CD8⁺ and CD4⁺ cells, respectively, in spleens of mice that received BALB/c BM and rIgG. Anti-ICOS reduced the number of donor BM-specific Tg CD8⁺ and CD4⁺ cells by 52% and 63%, respectively, indicating that in vivo ICOS blockade significantly inhibited, but did not abrogate, expansion of alloantigen-specific host T cells (Figure 5). Although ICOS blockade reduced the expansion of host antidonor T cells, it did not inhibit their activation (data not shown). These data indicating the inhibition of alloantigen-specific host T-cell expansion by ICOS blockade complement the data demonstrating increased engraftment in ICOS⁻/⁻ recipients. Together, these data indicate that the ICOS pathway plays a role in BM graft rejection.

Discussion

These studies indicate that the ICOS costimulatory pathway plays an important role in both donor antihost (GVHD) and host antidonor (rejection) alloresponses. ICOS blockade, achieved either through gene-deficient mice or the in vivo administration of anti-ICOS mAb, resulted in significant amelioration of GVHD in multiple strain combinations whether mediated by polyclonal CD4⁺ and/or CD8⁺ T cells; alloantigen-specific TCR Tg T cells, or CD28-, Th1-, or Th2-deficient T cells. Consistent with the known role of ICOS in regulation of T-cell responses after activation,[1] ICOS blockade inhibited in vivo alloreactive T-cell expansion but did not prevent T-cell activation or the generation of the cytotoxic effector molecule, granzyme B.[24] Imaging studies indicated that ICOS blockade resulted in striking reductions of GVHD effector cell infiltrations into the small intestine and skin with more modest or transient effects in other GVHD target organs. The differential results of ICOS blockade on organ infiltration suggest effects on T-cell homing and migration in addition to inhibition of T-cell expansion.

These studies used an established Tg model of GVHD in which BALB/c-reactive Tg (2C CD8⁺ and TEa CD4⁺) T cells were infused into irradiated CB6 recipients to allow for the study of donor antihost alloresponses.[19] Additionally, this paper describes a new Tg model of rejection in which B6 host-type, BALB/c-reactive Tg T cells were transferred into syngeneic B6 Rag⁻/⁻ recipients that were irradiated and given allogeneic BALB/c BM to allow for

Table 2. ICOS⁻/⁻ recipients have reduced graft-rejecting capacity

Donor	Host	6 wk		4 mo	
		No. chimeric	% Donor	No. chimeric	% Donor
BALB/c	B6 WT	11/20	29 ± 6	7/15	32 ± 11
BALB/c	B6 ICOS⁻/⁻	20/20*	61 ± 5*	14/14*	90 ± 4*

Host mice were sublethally irradiated on day 1 (5.5 Gy TBI) and infused with 10 × 10⁶ allogeneic TCD donor BM on day 0. PBLs were typed for percentage donor-host at 6 weeks and 4 months after BMT. Chimeric is defined as having more than 3% donor PBLs. Percentage donor is defined as average percentage donor cells of all mice in the group ± 1 SEM.

*P < .001 compared with B6 WT (pool of 2 experiments).

the study of host antidonor alloantigen-specific responses. Somewhat gratifying to us, ICOS blockade inhibited 2C CD8^{+} cells similarly in both models (63% inhibition in GVHD and 52% inhibition in rejection model; Figures 3B,5). The degree of inhibition mediated by ICOS blockade on TEa CD4^{+} cells was more variable (26% inhibition in GVHD and 63% inhibition in rejection model). This partial inhibition of T-cell expansion mediated by anti-ICOS mAb in a Tg model of GVHD was sufficient to result in a profound survival advantage (Figure 3A). GVHD inhibition by ICOS blockade (either by use of mAb or ICOS$^{-/-}$ donors) was confirmed in several different polyclonal models of GVHD. Although ICOS$^{-/-}$ mice had enhanced donor engraftment compared with WT mice, we cannot rule out possible contributions from non–T-cell mechanisms such as natural killer cell defects or reduced stem cell competition in ICOS$^{-/-}$ recipients. Therefore, the percent inhibition of expansion of adoptively transferred T cells in the Tg rejection model may not correlate perfectly with inhibition of graft rejection. Further studies to directly measure T-cell–mediated rejection in polyclonal models are warranted.

Imaging provides a vivid illustration of the widespread organ infiltration by effector T cells during GVHD.[18,22] Imaging data indicate that ICOS blockade resulted in an inhibition and/or delay in the expansion of effector T cells rather than an abrogation of priming, which might be expected to result in a more sustained reduction of GFP[+] effectors in all GVHD target organs. In addition to the inhibition of T-cell expansion, we hypothesize that ICOS blockade may have additional effects on T-cell homing and migration, as is evidenced by the profound and sustained reduction of GFP[+] effectors into the ileum and skin. These data illustrating the effect of ICOS blockade on GFP[+] effectors contrast with the effect of T regulatory cell infusions, which resulted in a more profound and sustained inhibition of GFP[+] effectors in a wider range of GVHD organs—a result thought to be due to inhibition of earlier events in the immune response.[18]

Of clinical interest, anti-ICOS significantly increased MST even when mAb infusions were delayed until day 5 after transplantation. Historically, delaying therapeutic intervention until day 5 has rarely led to GVHD inhibition of our models, likely due to the extent of priming and early expansion that has already occurred by this time.[22] Furthermore, in contrast to ICOS:ICOSL blockade, neither CD28:B7, CD40L:CD40, nor OX40:OX40L blockade extended survival time when antibodies were delayed until day 5 (data not shown, P.A.T.). The differential effect of ICOS on regulating effector responses make it an attractive candidate for combined blockade with the CD28:B7 or CD40L:CD40 pathway, both of which are more critical for initial activation events. Consistent with this, Nanji et al[11] found that combined blockade of ICOS with either CD40L:CD40 or CD28:B7 blockade resulted in enhanced islet allograft survival. Additionally, the role of ICOS in regulation of effector T cells after activation suggests that, in addition to GVHD therapy, ICOS blockade may be useful for the therapeutic targeting of primed or memory cells that are less likely to be governed by other costimulatory pathways.

Our results indicating GVHD inhibition by ICOS blockade in all of our models contrast somewhat with those of Ogawa et al.[12] They found that ICOS blockade accelerated acute GVHD and ameliorated chronic GVHD, effects postulated to be the result of selective inhibition of IL-4 production and Th1 polarization.[12] However, they used a nonirradiated parent-into-F1 GVHD model that may be more amenable to Th polarization by ICOS blockade, whereas all of our models involved host conditioning with total body irradiation. Consistent with this hypothesis, ICOS blockade during immune priming exacerbated experimental autoimmune encephalomyelitis that was thought to be due to Th1 polarization due to impairment of Th2 development.[25] In contrast and despite the fact that ICOS signaling preferentially induces IL-4 and IL-10,[1] our data indicate that ICOS blockade inhibited GVHD mediated by either STAT4$^{-/-}$ (Th1-deficient) or STAT6$^{-/-}$ (Th2-deficient) effectors (Figure 2B). However, a more profound effect on GVHD inhibition by ICOS blockade was observed with either WT or STAT4$^{-/-}$ donor splenocytes compared with STAT6$^{-/-}$ donor splenocytes, indicating a greater benefit on inhibiting Th2-mediated GVHD.

This study demonstrates that ICOS blockade had positive effects for GVHD inhibition, GVHD therapy, and allogeneic BM graft promotion. These data together with the intriguing report that ICOS expression most accurately defines inflammatory effector T cells[26] suggest that the ICOS pathway could be an important therapeutic target.

Acknowledgments

References

1. Hutloff A, Dittrich AM, Beier KC, et al. ICOS is an inducible T-cell co-stimulator structurally and functionally related to CD28. Nature. 1999;397:263-266.

2. Swallow MM, Wallin JJ, Sha WC. B7h, a novel costimulatory homolog of B7.1 and B7.2, is induced by TNFalpha. Immunity. 1999;11:423-432.

3. Gonzalo JA, Delaney T, Corcoran J, Goodearl A, Gutierrez-Ramos JC, Coyle AJ. Cutting edge: the related molecules CD28 and inducible costimulator deliver both unique and complementary signals required for optimal T cell activation. J Immunol. 2001;166:1-5.

4. Coyle AJ, Gutierrez-Ramos JC. The expanding B7 superfamily: increasing complexity in costimulatory signals regulating T cell function. Nat Immunol. 2001;2:203-209.

5. Dong C, Juedes AE, Temann UA, et al. ICOS costimulatory receptor is essential for T-cell activation and function. Nature. 2001;409:97-101.

6. McAdam AJ, Greenwald RJ, Levin MA, et al. ICOS is critical for CD40-mediated antibody class switching. Nature. 2001;409:102-105.

7. Mak TW, Shahinian A, Yoshinaga SK, et al. Co-stimulation through the inducible costimulator ligand is essential for both T helper and B cell functions in T cell-dependent B cell responses. Nat Immunol. 2003;4:765-772.

8. Nurieva RI, Mai XM, Forbush K, Bevan MJ, Dong C. B7h is required for T cell activation, differentiation, and effector function. Proc Natl Acad Sci U S A. 2003;100:14163-14168.

9. Harada H, Salama AD, Sho M, et al. The role of the ICOS-B7h T cell costimulatory pathway in transplantation immunity. J Clin Invest. 2003;112:234-243.

10. Guo L, Li XK, Funeshima N, et al. Prolonged survival in rat liver transplantation with mouse monoclonal antibody against an inducible costimulator (ICOS). Transplantation. 2002;73:1027-1032.

11. Nanji SA, Hancock WW, Anderson CC, et al. Multiple combination therapies involving blockade of ICOS/B7RP-1 costimulation facilitate long-term islet allograft survival. Am J Transplant. 2004;4:526-536.

12. Ogawa S, Nagamatsu G, Watanabe M, et al. Opposing effects of anti-activation-inducible lymphocyte-immunomodulatory molecule/inducible costimulator antibody on the development of acute versus chronic graft-versus-host disease. J Immunol. 2001;167:5741-5748.

13. Tafuri A, Shahinian A, Bladt F, et al. ICOS is essential for effective T-helper-cell responses. Nature. 2001;409:105-109.

14. Grubin CE, Kovats S, deRoos P, Rudensky AY. Deficient positive selection of CD4 T cells in mice displaying altered repertoires of MHC class II-bound self-peptides. Immunity. 1997;7:197-208.

15. Sha WC, Nelson CA, Newberry RD, Kranz DM, Russell JH, Loh DY. Positive and negative selection of an antigen receptor on T cells in transgenic mice. Nature. 1988;336:73-76.

16. Taylor PA, Lees CJ, Blazar BR. The infusion of ex vivo activated and expanded CD4(+)CD25(+)

immune regulatory cells inhibits graft-versus-host disease lethality. Blood. 2002;99:3493-3499.

17. Cohen JL, Trenado A, Vasey D, Klatzmann D, Salomon BL. CD4(+)CD25(+) immunoregulatory T cells: new therapeutics for graft-versus-host disease. J Exp Med. 2002;196:401-406.

18. Taylor PA, Panoskaltsis-Mortari A, Swedin JM, et al. L-Selectin[hi] but not the L-Selectin[lo] CD4+25+ T-regulatory cells are potent inhibitors of GVHD and BM graft rejection. Prepublished on August 3, 2004, as DOI 10.1182/blood-2004-05-1850. (Now available as Blood. 2004;104:3804-3812.)

19. Gonzalez M, Quezada SA, Blazar BR, Panoskaltsis-Mortari A, Rudensky AY, Noelle RJ. The balance between donor T cell anergy and suppression versus lethal graft-versus-host disease is determined by host conditioning. J Immunol. 2002;169:5581-5589.

20. Blazar BR, Taylor PA, McElmurry R, et al. Engraftment of severe combined immune deficient mice receiving allogeneic bone marrow via in utero or postnatal transfer. Blood. 1998;92:3949-3959.

21. Grossman WJ, Verbsky JW, Tollefsen BL, Kemper C, Atkinson JP, Ley TJ. Differential expression of granzymes A and B in human cytotoxic lymphocyte subsets and T regulatory cells. Prepublished on July 6, 2004, as DOI 10.1182/blood-2004-03-0859. (Now available as Blood. 2004; 104:2840-2848.)

22. Panoskaltsis-Mortari A, Price A, Hermanson JR, et al. In vivo imaging of graft-versus-host-disease in mice. Blood. 2004;103:3590-3598.

23. Nikolic B, Lee S, Bronson RT, Grusby MJ, Sykes M. Th1 and Th2 mediate acute graft-versus-host disease, each with distinct end-organ targets. J Clin Invest. 2000;105:1289-1298.

24. Graubert TA, Russell JH, Ley TJ. The role of granzyme B in murine models of acute graft-versus-host disease and graft rejection. Blood. 1996; 87:1232-1237.

25. Rottman JB, Smith T, Tonra JR, et al. The co-stimulatory molecule ICOS plays an important role in the immunopathogenesis of EAE. Nat Immunol. 2001;2:605-611.

26. Lohning M, Hutloff A, Kallinich T, et al. Expression of ICOS in vivo defines CD4+ effector T cells with high inflammatory potential and a strong bias for secretion of interleukin 10. J Exp Med. 2003;197: 181-193.